Title
Direct observation of delithiation as the origin of analog memristance in LixNbO2

Journal
APL Materials, 7(7)

ISSN
2166-532X

Authors
Howard, Sebastian A
Singh, Christopher N
Paez, Galo J
et al.

Publication Date
2019-07-01

DOI
10.1063/1.5108525

Peer reviewed

Direct observation of delithiation as the origin of the valence change memristance in Li_xNbO_2

Sebastian A. Howard,[1] Christopher N. Singh,[1] Galo J. Paez,[1] Matthew J. Wahila,[1] Linda W. Wangoh,[1] Shawn Sallis,[2] Keith Tirpak,[1] Yufeng Liang,[3] David Prendergast,[3] Mateusz Zuba,[1] Jatinkumar Rana,[1] Alex Weidenbach,[4] Timothy M. McCrone,[4] Wanli Yang,[5] Tien-Lin Lee,[6] Fanny Rodolakis,[7] William Doolittle,[4] Wei-Cheng Lee,[1] and Louis F. J. Piper[1, 2, a)]

[1)] *Department of Physics, Applied Physics and Astronomy, Binghamton University, Binghamton, New York 13902, USA*

[2)] *Materials Science & Engineering, Binghamton University, Binghamton, New York 13902, USA*

[3)] *The Molecular Foundry, Lawrence Berkeley National Laboratory, Berkeley, California 94720, USA*

[4)] *School of Electrical and Computer Engineering, Georgia Institute of Technology, Atlanta, GA, 30332, USA*

[5)] *Advanced Light Source, Lawrence Berkeley National Laboratory, Berkeley, California 94720, USA*

[6)] *Diamond Light Source Ltd., Harwell Science and Innovation Campus, Didcot, Oxfordshire OX11 0DE, UK*

[7)] *Argonne National Laboratory, 9700 South Cass Avenue, Argonne, IL 60439, USA*

(Dated: 29 April 2019)

The discovery of analog Li_xNbO_2 memristors revealed a promising new memristive mechanism wherein the diffusion of Li^+ rather than O^{2-} ions enables precise control of the resistive states. However, directly correlating lithium concentration with changes to the electronic structure in active layers remains a challenge and is required to truly understand the underlying physics. Chemically delithiated single crystals of $LiNbO_2$ present a model system for correlating lithium variation with spectroscopic signatures from operando soft x-ray spectroscopy studies of device active layers. Using electronic structure modeling of the x-ray spectroscopy of Li_xNbO_2 single crystals, we demonstrate that the intrinsic memristive behavior in Li_xNbO_2 active layers results from field-induced degenerate p-type doping. We show that electrical operation of Li_xNbO_2-based memristors is viable even at marginal Li deficiency and that the analog memristive switching occurs well before the system is fully metallic. This study serves as a benchmark for material synthesis and characterization of future Li_xNbO_2-based memristor devices, and suggests that valence change switching is a scalable alternative that circumvents the electroforming typically required for filamentary-based memristors.

Functional oxide memristors have the potential to revolutionize neuromorphic computing, which aims to mimic the operation of biological brains using artificial circuits.[1,2] While neuromorphic systems can be implemented with traditional CMOS circuitry, this requires a large number of conventional transistors, resulting in significant power consumption and scalability issues.[3–5] In contrast, truly biomimetic circuits would lead to scalable, low-power processors capable of hardware-level autonomous learning, power-efficient image recognition, and other exciting possibilities.[6,7] Neuristor circuits based on functional oxide memristors have the potential to enable these truly biomimetic circuits. However, the resistive switching of these memristors is typically attributed to a complex combination of processes (e.g., redox reactions, ionic transport, phase changes, etc.),[8] which are dependent on device architecture and are not yet fully understood.[9]

Lithium niobite (Li_xNbO_2), which has been previously studied for its interesting properties such as superconductivity,[10] has recently shown great potential for memristive applications.[11,12] Whereas traditional filamentary devices require the migration of O^{2-} ions to access discrete resistive states, the resistive states of Li_xNbO_2 are analog in nature and are thought to be modulated by the diffusion of Li^+ ions within the active layer.[13] It has been proposed that the electronic properties of Li_xNbO_2 are highly dependent on the Li^+ content, and that a voltage induced Li-gradient could enable precise control of the resistive state.[14] This voltage-induced Li gradient was previously investigated across an annular $LiNbO_2$ thin film device using spatially resolved in-situ O K-edge XAS,[13] revealing changes in the XAS lineshape across the active layer interpreted as lithium concentration variations. Recent advances in x-ray absorption simulations of the O K-edge[15] have now presented a opportunity to confirm the predicted evolution of Li_xNbO_2 within these devices and accurately describe their operational mechanism.

[a)] Electronic mail: lpiper@binghamton.edu

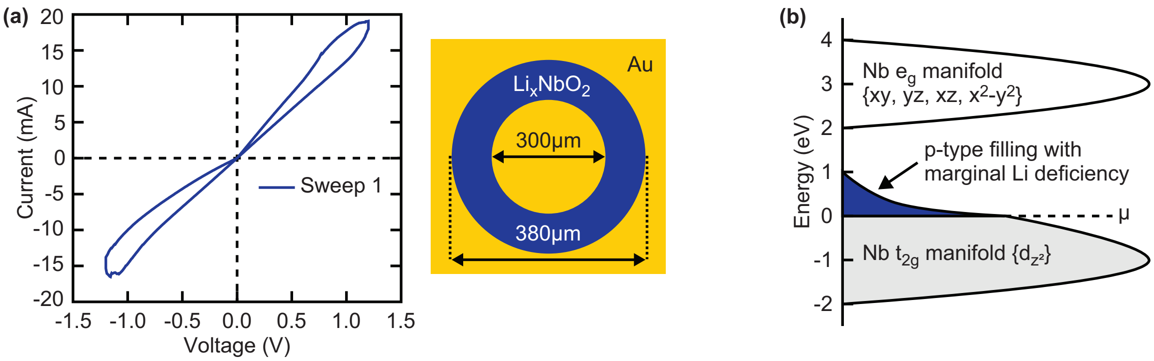

FIG. 1. **(a)** The IV Sweep (left) of a ring dot memristor device (right) fabricated using a Li_xNbO_2 crystal grown via liquid phase electro-epitaxy. **(b)** A schematic band diagram depicting the metal cation valence manifold reacting to Li deficiency. Oxygen 2p character forms only ≈ 10% of the bands at this energy, and so are omitted for clarity.

In this paper, we benchmark the intrinsic material properties responsible for the analog memristive behavior of Li_xNbO_2. High-quality single crystals were grown using liquid phase electro-epitaxy and then chemically delithiated for direct comparison to atomistic modeling. High quality Li_xNbO_2 single crystals with well-defined lithium concentrations were preferred over active layer thin films in order to disentangle the effects of Li content variation from other phenomenon. Soft and hard x-ray spectroscopy techniques, as well as first-principles x-ray spectroscopic simulations, were used to monitor the niobium coordination and electronic structure evolution of Li_xNbO_2. From O K-edge XAS, we were able to confirm the depopulation of the Nb 4d$_{z^2}$ orbital upon Li^+ ion extraction, considered responsible for the memristive behavior. From the excellent agreement between theory and experiment, we are able to explain the electronic structure evolution of Li_xNbO_2 up to $x = 0.5$, i.e., degenerate p-type semiconductor regime (above which the Li_xNbO_2 is metallic). From reexamining previous *in-situ* O K-edge XAS measurements of Li_xNbO_2,[13] we conclude that the linear memristive switching in the devices occurs within the degenerate p-doping regime rather than being associated with a full insulator-to-metal transition.

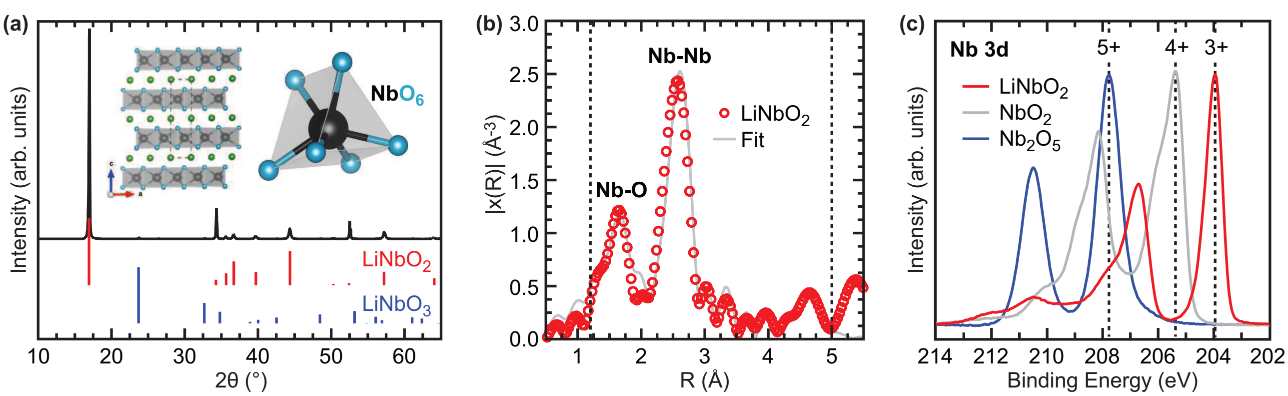

FIG. 2. **(a)** X-ray diffraction and **(b)** EXAFS fit. The fitting range is denoted by the dashed lines. **(c)** HAXPES (6 keV) of pristine $LiNbO_2$ single crystals compared with NbO_2 (Nb^{4+}) and Nb_2O_5 (Nb^{5+}) references, confirming the expected Nb^{3+} oxidation state of $LiNbO_2$. Dashed vertical lines indicate energetic positions of the Nb 3d$_{5/2}$ peak for each oxidation state.

$LiNbO_2$ single crystals were grown using a liquid phase electro-epitaxy (LPEE) method. The LPEE growth method makes use of Nb_2O_5 (99.9%) and $LiBO_2$ (99.9%). The $LiNbO_2$ crystals were grown over a 24 hour period and nucleated on a niobium rod at 1.1 V with a 10:1 $LiBO_2$ to Nb_2O_5 ratio. Some $LiNbO_2$ crystals were delithiated in a 37% HCl aqueous bath at room temperature for 24 hours followed by a rinse with DI water, and then dried with nitrogen. Other crystals were set aside to act as pristine references, while some large crystals were reserved for device fabrication. To create the memristor devices, 100 nm of Ti and 500 nm of Au were deposited on the large crystals using evaporation and then patterned into device contacts using a lift-off process. These volatile ring dot devices were then tested with IV sweeps. Initial scans were performed to find minimum programming voltage starting at 0.1 V and increasing in steps of 0.1 V, followed by a collection of data at minimum programming voltage.[16]

Some crystals were ball milled or ground manually using a mortar and pestle for powder measurements. X-ray diffraction (XRD) was performed on powderized $LiNbO_2$ using a Bruker D8 Advance diffractometer with Bragg-Brentano geometry and a Cu K_α source at Georgia Institute of Technology. Phase identification was performed using Bruker DIFFRAC.EVA software coupled with the PDF-2016 database. X-ray absorption near edge structure (XANES) and extended x-ray absorption fine structure (EXAFS) measurements were also performed on powderized $LiNbO_2$ to determine the effective Nb oxidation state in the bulk, as well as local electronic/atomic structure. The XANES and EXAFS were performed at beamline 20-BM of the Advanced Photon Source at Argonne National Laboratory in Lemont, IL (see section I A. of the supplementary material).

Soft and hard x-ray photoelectron spectroscopy (XPS and HAXPES), which have an effective probing depth of $\sim$ 4 nm (surface) and $\sim$ 15 nm (sub-surface), respectively, were performed on $LiNbO_2$ crystals to determine the Li content, Nb oxidation state, and the valence band electronic structure. In addition, x-ray absorption spectroscopy (XAS) measurements of the oxygen K-edge were performed in total electron yield (TEY) mode, which can probe up to 5 nm deep.[17] The HAXPES was performed at beamline I09 of the Diamond Light Source at the Harwell Science and Innovation Campus in Oxfordshire, UK, while variable photon energy XPS and XAS was performed at beamline 29-ID of the Advanced Photon Source at Argonne National Laboratory in Lemont, IL. Some additional XPS was performed at the Analytical and Diagnostics Laboratory at Binghamton University, while additional XAS was performed at beamline 8 of the Advanced Light Source at Lawrence Berkeley National Laboratory in Berkeley, CA (see sections I A and B. of the supplementary material).

Electronic ground state calculations at various Li concentrations were performed within the Vienna Ab Initio Simulation (VASP) package,[18] (see section I C. of the supplementary material).The x-ray formalism of the core-hole approach for simulating the O k-edge in pristine and delithiated cases was performed within the ShirleyXAS + MBX-ASPY environment.[15,19–21] The DFT information of the x-ray final state was obtained using full core-hole (FCH) approach in which an electron is removed from the inner shell of a designated excited atom within a supercell. Therefore, the interaction between the core hole and the electron was not explicitly included via many-body approaches, such as the Feynman diagram technique, but was instead accounted for using a modified oxygen pseudo-potential with one electron removed from the 1s orbital for the O K-edge. The excited electron was then added to the occupied electronic structure. Next, the modified electronic system was relaxed to its ground state using DFT. Finally, the initial-state and final-state DFT orbitals and energies were provided as input for the MBXASPY software codes to produce the determinant spectra. We utilized a $1 \times 1 \times 1$ supercell structure for the rutile and BCT NbO_2 calculations, as well as the $Li_{0.5}NbO_2$. The fully lithiated $LiNbO_2$ was calculated using a $3 \times 3 \times 1$ supercell. All supercells were chosen such that their dimensions were large enough to avoid effects due to neighboring periodic images

A representative pinched hysteresis IV curve taken on a high-quality, single crystal $LiNbO_2$ ring dot memristor is shown in Figure 1(a), consistent with previous reports of analog memristive behavior for $LiNbO_2$.[16,22] Since the crystals show similar IV curve responses to $LiNbO_2$ devices grown via both molecular beam epitaxy[11,13] and sputter deposition[23], we consider the underlying mechanism to be inherent to the material rather than the device processing. As such, chemically delithiated $LiNbO_2$ single crystals should display the same electronic structure modifications as those electrochemically induced in the thin film devices. As shown in Figure 1(b), the chemical potential (μ) is expected to lower into the Nb $4d_{z^2}$-derived valance band as lithium is extracted, thereby favoring hole formation (p-type). Although the Nb-O bond length and O K-edge XAS lineshape are reportedly sensitive to d_{z^2} occupancy,[13,14,24] direct measurement of Li concentration combined with accurate simulations of the O K-edge XAS are required to fully verify the electronic structure evolution of Li_xNbO_2 and understand the memristive mechanism.

To evaluate the quality of our pristine $LiNbO_2$ crystals, powder x-ray diffraction (XRD) was performed. Figure 2(a) shows the hexagonal $P6_3/mmc$ crystal structure (inset) and XRD pattern of our $LiNbO_2$ powder with the reflections indexed with PDF 029-0815. The XRD pattern predominantly shows the expected structure with some negligible contribution from $LiNbO_3$ impurities, which were likely introduced during the powder preparation process. XPS studies confirmed that these impurities were mainly limited to the crystal surface and could be reduced by exposing fresh crystal surfaces using a razor blade (see section II A. of the supplementary material). Henceforth, all results shown were taken on carefully cleaved samples and/or measured using bulk-sensitive techniques to avoid spectral contamination from over-oxidized surface species.

Bulk-sensitive extended x-ray absorption fine structure (EXAFS) of lithium niobite ground pellets was performed to confirm the local atomic structure, shown in Figure 2(b). The data was fit using the $LiNbO_2$ crystal structure from the materials project database (ICSD-451)[25] (see section II B. of the supplementary materials). The first peak around 1.654 Åcorresponds to the Nb-O interaction in the first coordination shell, while the second peak around 2.596 Åis due to the Nb-Nb interaction in the second coordination shell. Excellent agreement between the experimental data and theory is achieved up to $\sim$5 Å. Taken together, the XRD and EXAFS results confirm the overall phase purity of our $LiNbO_2$ crystals.

HAXPES was then employed to confirm the bulk Nb oxidation states of our lithium niobite crystals, shown in Figure 2(c). NbO_2 and Nb_2O_5 thin films are used as Nb^{4+} and Nb^{5+} oxidation state references. The Nb 3d spectra consists of two distinct spin-split peaks ($3d_{5/2}$ and $3d_{3/2}$), with the energetic positions of the primary $3d_{5/2}$ peak at

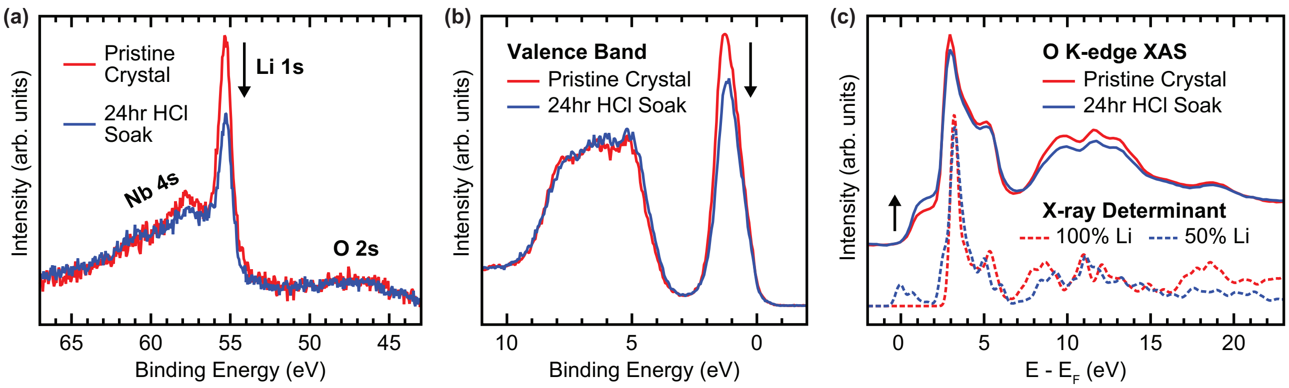

FIG. 3. Soft XPS of the **(a)** Li 1s core level and **(b)** valence band region, as well as **(c)** TEY mode O K-edge XAS compared with x-ray determinant approach simulations for pristine and 24 hour HCL soaked $LiNbO_2$ crystals.

204.1 eV, 206.7, and 207.3 for Nb^{3+}, Nb^{4+} and Nb^{5+}, respectively.[26–32] Our pristine $LiNbO_2$ displays no evidence of Nb^{4+}, however, it does display a weak Nb^{5+}-like component consistent with there being an over-oxidized $LiNbO_3$ surface.

The effect of chemical delthiation on the electronic structure of $LiNbO_2$ was studied via XPS and XAS, as shown in Figure 3. The lower photon energy ($h\nu = 700$ eV) used for the XPS results in a higher Li 1s photo-ionization cross section than is possible with a traditional laboratory-based XPS system, thus improving our sensitivity to variations in Li content associated with delithiation (see section II C. of the supplementary materials). After the crystal was soaked for 24 hours in an HCl bath, a drop in the Li 1s peak intensity is observed in Figure 3(a), associated with a reduction in bulk Li content. This delithiation is accompanied by a compensating change to a higher Nb oxidation state observed in both the Nb 4s and 3d core regions, as well as a reduced Nb-O bond length in EXAFS fitting and a shifted Nb K-edge XANES spectra (see section II B. of the supplementary materials). This delithiation also results in the depopulation of Nb states near the Fermi level, as shown in Figure 3(b). Importantly, the lack of a clear Fermi edge upon delithiation indicates that the material stays within *p*-type semiconductor regime, i.e., not fully metallic.

Figure 3(c) shows experimental O K-edge spectra taken using TEY mode XAS and simulations of the O K-edge calculated using the x-ray formalism of the core-hole approach.[19] One feature that clearly changes with lithium content is a pre-edge feature located around 1 - 2 eV, which is found to increase in intensity with delithiation. While simulations show a complete lack of this pre-edge feature at 100% lithiation, our pristine experimental spectra still displays some weight at this energy, indicating the pristine single crystals may not possess a 100% lithium concentration. It is important to note that our O K-edge lineshapes are in agreement with those previously reported by Greenlee et al. from spatially resolved in-situ O K-edge XAS of $LiNbO_2$ devices. This suggests that perfectly stoichiometric $LiNbO_2$ is not necessary to achieve a memristive response.[13] Additionally, the trends Greenlee et al. observed across their device from the positive to negative electrode matches our observed changes with delithiation, confirming that changing Li content produces the observed analog memristive response.

Additional computational methods were used to qualitatively estimate the regime of p-type doping observed in our samples. Figure 4 shows the projected density of states of Li_xNbO_2 as a function of Li content. Starting with the stoichiometric x = 100% case, the semiconducting gap is inside the Nb *d* manifold of ∼1.5 eV. While the experimental gap is closer to 2 eV[14], this is consistent with other theoretical predictions[24,33] and the general tendency of LDA methods to under-estimate gap strengths. Looking at the first principles simulations for delithitated cases (x < 100%), we can now clarify the electronic response without assuming a rigid band model. As Li is driven out of the system, there is a clear auto-doping effect where the top of the valence band is heavily *p*-doped as previously reported,[14] however we also notice that the curvature of the bands is still high at marginal delithitation and only flattens out upon deeper delithiation. Formation of light hole states, namely depopulation of d_{z^2} observed in operando O K-edge XAS,[13] can give rise to the low field linear memristive response before truly metallic behavior sets in. Figure 4 reveals that the onset of a divergent dielectric function at $Li_{0.5}NbO_2$ (see section II D. of the supplementary material), meaning that metallicity doesn't occur until nearly 50% delithitation. By comparing the measured valence band (Fig. 3(b)) to simulations and to operando XAS studies of active layers, we conclude that the memristive response is due to lithium variation within the *p*-type semiconductor (marginal delithitation) regime. In light of this, we determine that the memristive response does not require the metallic phase, suggesting that the dominant turn-on effect is the formation of light *p*-carriers.

The analog memristive behavior observed to Li_xNbO_2 single crystals has been investigated with a variety of experimental and theoretical techniques. We show intrinsic memristive behavior in lithium niobite phase pure single

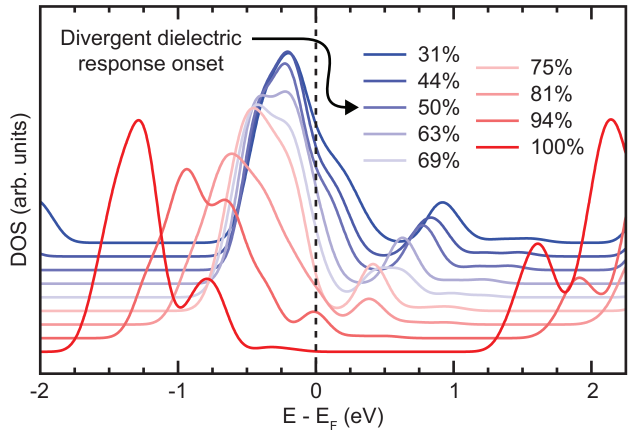

FIG. 4. Evolution of the density of states as function of x in Li_xNbO_2. A continuously increasing hole population was observed with decreasing Li.

crystals, and use chemical delithiation of these crystals to benchmark the resulting electronic structure changes. We show that removal of Li oxidizes the Nb and thus depopulates the top Nb d-states within the valence band, facilitating early onset p-type conduction prior to metallicity. This work clarifies that the field driven Li-ion motion inherent to Li_xNbO_2 is a viable analog switching mechanism that does not require any complex interfacial effects or pre-forming/electroforming.

ACKNOWLEDGMENTS

This material is based upon work supported by the Air Force Office of Scientific Research under award number FA9550–18–1–0024. Galo J. Paez acknowledges doctoral degree grant support from the Fulbright Foreign Student Program (Grant ID: E0565514) and Keith Tirpak was supported by a NSF-REU (NSF DMR-1658990). We acknowledge Diamond Light Source for time on Beamline I09 under Proposals SI20647. This research used resources of the Center for Functional Nanomaterials and the National Synchrotron Light Source II, which are U.S. Department of Energy (DOE) Office of Science facilities at Brookhaven National Laboratory, under Contract No. DE-SC0012704. This research used resources of the Advanced Light Source and the Molecular Foundry, which are U.S. DOE Office of Science facilities at Lawrence Berkeley National Laboratory under Contract No. DE-AC02-05CH11231. This research used resources of the Advanced Photon Source, a U.S. DOE Office of Science User Facility operated for the DOE Office of Science by Argonne National Laboratory under Contract No. DE-AC02-06CH11357; additional support by National Science Foundation under Grant no. DMR-0703406.

[1] T. Prodromakis and C. Toumazou, "A review on memristive devices and applications." in *ICECS* (2010) pp. 934–937.
[2] C. Sung, H. Hwang, and I. K. Yoo, "Perspective: A review on memristive hardware for neuromorphic computation," Journal of Applied Physics **124**, 151903 (2018).
[3] E. Chicca, G. Indiveri, and R. Douglas, "An adaptive silicon synapse," in *Proceedings of the 2003 International Symposium on Circuits and Systems, 2003. ISCAS '03.* (IEEE, 2003).
[4] W. M. Holt, "1.1 Moore's law: A path going forward," in *Solid-State Circuits Conference (ISSCC), 2016 IEEE International* (IEEE, 2016) pp. 8–13.
[5] Y. Li, Z. Wang, R. Midya, Q. Xia, and J. J. Yang, "Review of memristor devices in neuromorphic computing: materials sciences and device challenges," Journal of Physics D: Applied Physics **51**, 503002 (2018).
[6] D. Kuzum, S. Yu, and H. P. Wong, "Synaptic electronics: materials, devices and applications," Nanotechnology **24**, 382001 (2013).
[7] I. A. Young and D. E. Nikonov, "Principles and trends in quantum nano-electronics and nano-magnetics for beyond-CMOS computing," in *Solid-State Device Research Conference (ESSDERC), 2017 47th European* (IEEE, 2017) pp. 1–5.
[8] J. J. Yang, M. D. Pickett, X. Li, D. A. Ohlberg, D. R. Stewart, and R. S. Williams, "Memristive switching mechanism for metal/oxide/metal nanodevices," Nature nanotechnology **3**, 429 (2008).
[9] J. J. Yang, D. B. Strukov, and D. R. Stewart, "Memristive devices for computing," Nature nanotechnology **8**, 13 (2013).
[10] M. J. Geselbracht, T. J. Richardson, and A. M. Stacy, "Superconductivity in the layered compound Li_xNbO_2," Nature **345**, 324 (1990).
[11] J. D. Greenlee, W. L. Calley, W. Henderson, and W. A. Doolittle, "Halide based mbe of crystalline metals and oxides," physica status solidi c **9**, 155–160 (2012), https://onlinelibrary.wiley.com/doi/pdf/10.1002/pssc.201100468.
[12] J. D. Greenlee, W. L. Calley, M. W. Moseley, and W. A. Doolittle, "Comparison of interfacial and bulk ionic motion in analog memristors," IEEE Transactions on Electron Devices **60**, 427–432 (2013).
[13] J. D. Greenlee, C. F. Petersburg, W. Laws Calley, C. Jaye, D. A. Fischer, F. M. Alamgir, and W. Alan Doolittle, "In-situ oxygen x-ray absorption spectroscopy investigation of the resistance modulation mechanism in $LiNbO_2$ memristors," Applied Physics Letters **100**, 182106 (2012).

[14]J. C. Shank, M. B. Tellekamp, and W. A. Doolittle, "Evidence of ion intercalation mediated band structure modification and opto-ionic coupling in lithium niobite," Journal of Applied Physics **117**, 035704 (2015).
[15]Y. Liang and D. Prendergast, "Quantum many-body effects in x-ray spectra efficiently computed using a basic graph algorithm," Phys. Rev. B **97**, 205127 (2018).
[16]J. D. Greenlee, J. C. Shank, M. B. Tellekamp, B. P. Gunning, C. A. Fabien, and W. A. Doolittle, "Liquid phase electro-epitaxy of memristive $LiNbO_2$ crystals," Crystal Growth & Design **14**, 2218–2222 (2014).
[17]F. Lin, I. M. Markus, D. Nordlund, T.-C. Weng, M. D. Asta, H. L. Xin, and M. M. Doeff, "Surface reconstruction and chemical evolution of stoichiometric layered cathode materials for lithium-ion batteries," Nature communications **5**, 3529 (2014).
[18]G. Kresse and J. Furthmüller, "Efficient iterative schemes for ab initio total-energy calculations using a plane-wave basis set," Phys. Rev. B **54**, 11169–11186 (1996).
[19]Y. Liang, J. Vinson, S. Pemmaraju, W. S. Drisdell, E. L. Shirley, and D. Prendergast, "Accurate X-Ray Spectral Predictions: An Advanced Self-Consistent-Field Approach Inspired by Many-Body Perturbation Theory," Phys. Rev. Lett. **118**, 096402 (2017).
[20]P. Giannozzi, S. Baroni, N. Bonini, M. Calandra, R. Car, C. Cavazzoni, D. Ceresoli, G. L. Chiarotti, M. Cococcioni, I. Dabo, A. Dal Corso, S. de Gironcoli, S. Fabris, G. Fratesi, R. Gebauer, U. Gerstmann, C. Gougoussis, A. Kokalj, M. Lazzeri, L. Martin-Samos, N. Marzari, F. Mauri, R. Mazzarello, S. Paolini, A. Pasquarello, L. Paulatto, C. Sbraccia, S. Scandolo, G. Sclauzero, A. P. Seitsonen, A. Smogunov, P. Umari, and R. M. Wentzcovitch, "QUANTUM ESPRESSO: a modular and open-source software project for quantum simulations of materials," Journal of Physics: Condensed Matter **21**, 395502 (2009).
[21]P. Giannozzi, O. Andreussi, T. Brumme, O. Bunau, M. B. Nardelli, M. Calandra, R. Car, C. Cavazzoni, D. Ceresoli, M. Cococcioni, N. Colonna, I. Carnimeo, A. D. Corso, S. de Gironcoli, P. Delugas, R. A. D. Jr, A. Ferretti, A. Floris, G. Fratesi, G. Fugallo, R. Gebauer, U. Gerstmann, F. Giustino, T. Gorni, J. Jia, M. Kawamura, H.-Y. Ko, A. Kokalj, E. Kkbenli, M. Lazzeri, M. Marsili, N. Marzari, F. Mauri, N. L. Nguyen, H.-V. Nguyen, A. O. de-la Roza, L. Paulatto, S. Ponc, D. Rocca, R. Sabatini, B. Santra, M. Schlipf, A. P. Seitsonen, A. Smogunov, I. Timrov, T. Thonhauser, P. Umari, N. Vast, X. Wu, and S. Baroni, "Advanced capabilities for materials modelling with QUANTUM ESPRESSO," Journal of Physics: Condensed Matter **29**, 465901 (2017).
[22]J. D. Greenlee, J. C. Shank, M. B. Tellekamp, E. X. Zhang, J. Bi, D. M. Fleetwood, M. L. Alles, R. D. Schrimpf, and W. A. Doolittle, "Radiation effects on LiNbO2 memristors for neuromorphic computing applications," IEEE Transactions on Nuclear Science **60**, 4555–4562 (2013).
[23]J. C. Shank, M. B. Tellekamp, and W. A. Doolittle, "The crystallization and properties of sputter deposited lithium niobite," Thin Solid Films **609**, 6 – 11 (2016).
[24]E. R. Ylvisaker and W. E. Pickett, "First-principles study of the electronic and vibrational properties of $LiNbO_2$," Physical Review B **74**, 075104 (2006).
[25]A. Jain, S. P. Ong, G. Hautier, W. Chen, W. D. Richards, S. Dacek, S. Cholia, D. Gunter, D. Skinner, G. Ceder, and K. a. Persson, "The Materials Project: A materials genome approach to accelerating materials innovation," APL Materials **1**, 011002 (2013).
[26]I. Goldfarb, D. Ohlberg, J. Strachan, M. Pickett, J. J. Yang, G. Medeiros-Ribeiro, and R. Williams, "Band offsets in transition-metal oxide heterostructures," Journal of Physics D: Applied Physics **46**, 295303 (2013).
[27]X. Jia, L. Kang, X. Liu, Z. Wang, B. Jin, S. Mi, J. Chen, W. Xu, P. Wu, *et al.*, "High performance ultra-thin niobium films for superconducting hot-electron devices," IEEE Trans. Appl. Supercond **23**, 2300704–2300704 (2013).
[28]Y. Wang, R. B. Comes, S. Kittiwatanakul, S. A. Wolf, and J. Lu, "Epitaxial niobium dioxide thin films by reactive-biased target ion beam deposition," Journal of Vacuum Science & Technology A: Vacuum, Surfaces, and Films **33**, 021516 (2015).
[29]Q.-Y. Hao, B.-C. Zhu, D.-K. Wang, S.-Y. Zeng, Z. Gao, Y.-W. Hu, Y. Wang, Y.-K. Wang, and K.-B. Tang, "A New Potassium Intercalation Compound of 3R-$Nb_{1.1}S_2$ and its Superconducting Hydrated Derivative Synthesized via Soft Chemistry Strategy," Chemistry Select **1**, 2610–2616 (2016).
[30]C. Dong, X. Wang, X. Liu, X. Yuan, W. Dong, H. Cui, Y. Duan, and F. Huang, "In situ grown Nb_4N_5 nanocrystal on nitrogen-doped graphene as a novel anode for lithium ion battery," RSC Advances **6**, 81290–81295 (2016).
[31]J. C. Shank, M. B. Tellekamp, M. J. Wahila, S. Howard, A. S. Weidenbach, B. Zivasatienraj, L. F. Piper, and W. A. Doolittle, "Scalable Memdiodes Exhibiting Rectification and Hysteresis for Neuromorphic Computing," Scientific reports **8**, 12935 (2018).
[32]S. B. Basuvalingam, B. Macco, H. C. Knoops, J. Melskens, W. M. Kessels, and A. A. Bol, "Comparison of thermal and plasma-enhanced atomic layer deposition of niobium oxide thin films," Journal of Vacuum Science & Technology A: Vacuum, Surfaces, and Films **36**, 041503 (2018).
[33]D. L. Novikov, V. A. Gubanov, V. G. Zubkov, and A. J. Freeman, "Electronic structure and electron-phonon interactions in layered Li_xNbO_2 and Na_xNbO_2," Phys. Rev. B **49**, 15830–15835 (1994).